Dielectric Relaxation Behavior of Styrene–Isoprene Diblock Copolymers: Bulk Systems

Ming-Long Yao, Hiroshi Watanabe, Keiichiro Adachi, and Tadao Kotaka*

Department of Macromolecular Science, Faculty of Science, Osaka University, Toyonaka, Osaka 560, Japan

Received September 24, 1990; Revised Manuscript Received December 18, 1990

ABSTRACT: Dielectric relaxation of polystyrene–polyisoprene (SI) diblock copolymers was examined in the bulk state at low temperatures. Under such conditions microphase separation took place and PS blocks form glassy domains, and thus only the motion of PI blocks anchored on the domain boundary and confined in their own lamellae was observable. The dielectric normal modes of such end-grafted PI blocks due to their global motion were seriously affected by the confinements in microdomains: The normal modes were significantly retarded and broadened as compared to those of free homo-PI chains. To interpret such differences, spatial confinement as well as thermodynamic confinement (to keep uniform segment density) in microdomains was considered. Comparison of the normal modes between block- and homo-PI chains both mixed with (dielectrically inert) polybutadiene blocks in lamellae suggested that the effects of the confinements were interdependent and much larger for PI blocks than for homo-PI chains, probably because the requirement of uniform density affects the chain configuration much more seriously for the former with fixed ends than for the latter without such ends.

I. Introduction

It is well understood that the *microdomain* structure formed in a block copolymer of two immiscible polymers is a result of a compromise among some contradicting thermodynamic requirements characteristic of the block chains *confined* in such microdomains:[1-3] the tendency of segregation to reduce the interfacial area; the tendency to delocalize the block junctions to broaden the interphase; the tendency of the block chains to assume random configuration as much as possible; and finally the most deterministic requirement of the uniform overall segment density distribution throughout the interphase and microdomains. The morphological features of such microphase-separated block copolymers have been extensively studied and summarized as Molau's rule.[1,4]

The microdomain structure in a block copolymer obviously exerts profound influence on its physical properties such as rheological properties at *long* time scales.[5,6] When a small strain is imposed on such a block copolymer system so that the resulting stress is small and the microdomain structure is preserved, the system exhibits an elastic response. The restoring force reflects the distortion of block-chain configurations due to the external strain. For such a case, we essentially observe through the slow rheological response the effect of the thermodynamic forces on the static configuration of the confined block chains.[6]

In addition to the static effect mentioned above, we naturally expect that the thermodynamic forces should exert influence on the molecular motion of the confined block chains. Such a dynamic effect can be examined in principle through rheological measurement at short time scales. However, if the stress resulting from the deformation of the microdomain structure overwhelms those due to the molecular motion of the blocks, the viscoelastic spectroscopy alone may not provide clear-cut information on the motion of the block chains. Thus it would be convenient if we have a technique of observing the molecular motion alone that complements the viscoelastic spectroscopy.

If a polymer chain has the component of dipoles aligned in the same direction parallel to the chain contour, its global motion induces changes in polarization of the system, which can be detected dielectrically. We call such a chain the *type-A* chain, according to Stockmayer,[7] and the process, the dielectric *normal-mode* process.[8-14] The dielectric spectroscopy on type-A chains was pioneered a long time ago by Stockmayer[7] and has been extensively studied by Adachi, Kotaka, and co-workers.[8-14] For type-A chains, only *fluctuation* of the end-to-end vector around an average, i.e., only the time-dependent part accompanied by the global molecular motion, is observed. Thus, for block copolymers containing type-A blocks, the dielectric spectroscopy can be a powerful tool (complementary to the viscoelastic spectroscopy) for investigating the molecular motion of the particular blocks.

On the basis of the above idea, we examined diblock copolymers containing *cis*-polyisoprene (*cis*-PI) blocks as type-A segments. Specifically, differences between the behavior of homo- and block-PI chains were examined. In this paper, we present the results, emphasizing the effects of thermodynamic interactions on the large-scale motion of confined block chains in the microdomains.

II. Experimental Section

Materials: Four polystyrene–polyisoprene (SI) diblock copolymer samples were prepared via anionic living polymerization using a high-vacuum technique. First, a small fraction of a prescribed amount of isoprene (I) monomer was reacted in *n*-heptane with *sec*-butyllithium for 20 min at 60 °C (a seeding reaction). Then the remaining monomer was introduced and allowed to polymerize at room temperature for 48 h to obtain precursor polyisoprenyl anions. Under this condition we were able to obtain narrow molecular weight distribution *cis*-PI's with high cis content (≅75%). After this first step was completed, an aliquot was taken to recover precursor homo-PI for the later characterization. Most of the solvent, *n*-heptane, was then replaced by benzene through vacuum distillation, and a prescribed amount of styrene (S) monomer was introduced and allowed to react with the living polyisoprenyl anions. The polymerization solvent had to be exchanged, because *n*-heptane, essential to obtain high cis-content PI blocks, is a nonsolvent for PS blocks. After 48 h of reaction at room temperature, the resulting SI block anions were terminated with methanol to recover the block copolymer. The crude product was precipitated in methanol to remove (ionic) impurities, dissolved in benzene again, and freeze-dried and stored in vacuo until use.

For comparison, a polystyrene–polybutadiene (SB) diblock copolymer was also prepared via anionic living polymerization with *sec*-BuLi in benzene. For that sample, living polystyrenyl

0024-9297/91/2224-2955$02.50/0

Table I
Characteristics of Polymer Samples

code	$10^{-3}M_w$	M_w/M_n	ϕ_S, %
	SI Diblock Copolymers		
SI(5.3–4.6)	9.9	1.05	53.6
SI(12.5–9.5)	22.0	1.06	55.2
SI(14–14)	28.0	1.06	50.6
SI(42–42)	84.0	1.06	49.4
	PI Precursors		
PI(4.6)	4.6	1.05	
PI(9.5)	9.5	1.06	
PI(14)	14.0	1.06	
PI(42)	42.0	1.06	
	SB Diblock Copolymer		
SB(8.6–8.5)	17.1	1.08	50.5
	Homopolystyrene		
PS(10)[a]	10.5	1.08	100

[a] Supplied from the Tosoh Co.

anions were first prepared in benzene, and butadiene monomer was added afterward.

The SI and SB samples were characterized on a gel permeation chromatograph (GPC; Tosoh Co., Model HLC-801A) equipped with a triple detector system consisting of a UV-absorption monitor (Tosoh, Model UV-8), a low-angle laser light scattering photometer (Tosoh, Model LS-8000), and a built-in refractomer. Chloroform was the elution solvent, and, whenever necessary, commercially available monodisperse polystyrenes (Tosoh, TSK PS's) were used as elution standards.

Table I summarizes the molecular characteristics of the samples used in this study. All samples have narrow molecular weight distribution ($M_w/M_n < 1.1$). The code numbers indicate the molecular weights of the constituent blocks in the unit of thousands. For example, SI(12.5–9.5) indicates an SI diblock copolymer with the molecular weights of PS and PI blocks being 12.5×10^3 and 9.5×10^3, respectively. All SI and SB samples have approximately the same styrene content close to 50%.

Dielectric measurements: Dielectric measurements were made on bulk films of the SI block copolymers listed in Table I. For comparison, measurements were also made on films of the SB copolymer, SI/SB binary blends, PI/PS/SB ternary blends, and precursor homo-PI's.

All measurements were made with a transformer bridge (General Radio 1615A) in the range of frequencies from 20 Hz to 50 kHz and in the temperature range 200–410 K. The details were described elsewhere.[13] For most of the cases, the time–temperature superposition principle was valid at low temperatures, and we were able to construct master curves for the dielectric loss factor ϵ''.

Films of the copolymers and blends were prepared by casting from benzene solution directly on the electrode in a dielectric capacitance cell. The composition of these films was always carefully adjusted so that the (PI + PB)/PS composition was close to 50/50. Because benzene is a common good solvent for PS and PI (and PB) blocks, alternating lamellar phases parallel to the electrode surface were expected to be formed in the cast films.[1,4] After thorough removal of the solvent, the film was annealed in situ at 373 K under vacuum for 1 h to achieve an equilibrium morphology and then allowed to cool slowly to room temperature. Finally the cell was filled with helium to avoid moisture and degradative oxidization of diene blocks during measurements at high temperatures. Homo-PI samples were viscous liquids so that they were directly charged in the dielectric cell, and the high-temperature annealing was omitted.

III. Molecular Motion and Dielectric Response

The dielectric loss factor, $\epsilon''(f)$, at a frequency f is related to the autocorrelation function, $\Phi(t)$, of the system by[15]

$$\epsilon'' = -\Delta\epsilon \int_0^\infty \dot{\Phi}(t) \sin 2\pi f t \, dt \qquad (1)$$

where the dot indicates the time derivative, and $\Delta\epsilon$ is the relaxation intensity.

For the dielectric response observed with a pair of electrodes parallel to the xy plane, $\Phi(t)$ is related to the z-component of the polarization of the system $P_z(t)$

$$\Phi(t) = \frac{\langle P_z(t)\, P_z(0)\rangle}{\langle P_z(0)\, P_z(0)\rangle} \qquad (2)$$

where $\langle P_z P_z\rangle$ indicates an average for the product of P_z. The P_z has a stochastic nature, and all molecular motions leading to changes in $P_z(t)$ contribute to ϵ''.

For the dielectric response of SI (and SB) block copolymers in the frequency and temperature ranges examined in this paper, two types of motion have to be considered: One is the local motion, called the *segmental mode*, for which the changes in the component of dipoles perpendicular to the chain contour (type-B dipoles according to Stockmayer[7]) are detected; and the other is the global motion of *cis*-PI chains, leading to the dielectric normal-mode process due to the type-A dipoles.

Both PS and PI (or PB) blocks possess type-B dipoles and thus exhibit the segmental-mode process. This process is related to the glass transition and thus independent of the molecular weight for sufficiently long chains. On the other hand, only *cis*-PI blocks possess type-A dipoles also, and fluctuation of the block junction-to-end vector induces changes in polarization to exhibit the dielectric normal-mode process.

For the normal-mode process of PI blocks confined in lamellar domains parallel to the electrodes, P_z is proportional to a sum of the z-components of the end-to-end vectors of the blocks involved. The time derivative of the autocorrelation function of P_z appearing in eq 1 is then written as

$$\dot{\Phi}(t) = A^{-1} \sum_p \sum_q \sum_n \sum_m \langle \dot{z}_{n,p}(t)\, z_{m,q}(0)\rangle \qquad (3)$$

$$A = \sum_p \sum_q \sum_n \sum_m \langle z_{n,p}(0)\, z_{m,q}(0)\rangle \qquad (3')$$

where $z_{n,p}(t)$ is the z-component of the nth bond vector of the pth chain at time t. If no correlation exists between the different chains, the average of the cross product in eq 3, $\langle \dot{z}_{n,p} z_{m,q}\rangle$ with $p \neq q$, vanishes and eq 3 is simplified to

$$\dot{\Phi}(t) = A^{-1} \sum_p \sum_n \sum_m \langle \dot{z}_{n,p}(t)\, z_{m,p}(0)\rangle \qquad (4)$$

For an isolated PI chain at infinite dilution, eq 3 is simplified to eq 4 because of no correlation between two chains separated far away. For homo-PI chains in concentrated systems, Adachi and Kotaka[11,13] found that the relaxation intensity per chain is proportional to the weight-average molecular weight and thus to the mean-square end-to-end distance. This suggests that eq 3 is simplified to eq 4 also for such cases. The cross product, $\dot{z}_{n,p}(t)\, z_{m,q}(0)$ with $p \neq q$ in eq 3, appears to assume positive and negative values with the same probability, and hence its average vanishes. However, it is not clear whether eq 3 can be simplified to eq 4 also for the confined PI blocks or not, because the thermodynamic interactions exist for these block chains to correlate static configuration of the different blocks. We will later examine this point experimentally in more detail.

IV. Results and Discussion

IV-1. Temperature dependence of ϵ'' of SI copolymers: Measurements of ϵ'' at a constant frequency f with increasing temperature are convenient to specify

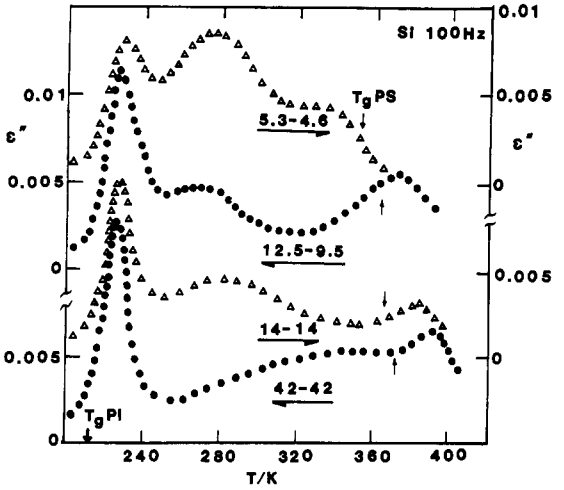

Figure 1. Temperature dependence of the dielectric loss factor ϵ'' for four SI copolymer samples indicated. The arrows indicate the glass transition temperatures for the PS and PI blocks involved.

dominant relaxation modes *in a qualitative sense*. Figure 1 shows results of such measurements on four SI samples listed in Table I. The frequency was 100 Hz, and the heating rate, 0.5 deg/min. For the sake of easy comparison, the origin for the vertical axis is shifted successively by a factor 0.005 for each sample.

As shown in Figure 1, the SI samples exhibit three prominent peaks in the ϵ'' curves. For each sample, the peak at the highest temperature reflects the segmental mode of PS blocks. The arrows indicate the glass transition temperature T_g^{PS} of PS blocks estimated from the PS block molecular weight M_{PS} by the Allen–Fox equation:[16]

$$1/T_g^{PS} = 1/373 + 0.72/M_{PS} \quad \text{in K}^{-1} \tag{5}$$

Loss maxima found in dynamic measurements are usually located at temperatures somewhat higher than the T_g^{PS} determined by a static method. This seems to be the case for the three high molecular weight SI copolymers, for which little mixing of PS and PI blocks is expected. On the other hand, for the lowest molecular weight SI(5.3–4.6) sample, the loss maximum temperature is somewhat lower than T_g^{PS}, suggesting partial mixing of PS and PI blocks in the interphase. However, it should be emphasized that even the structure of such a diffuse interphase would not change with T as long as the segmental motion of PS blocks is frozen at $T < T_g^{PS}$.

The peak at the lowest temperature can be attributed to the segmental mode of PI blocks: The peak location is insensitive to the PI block molecular weight M_{PI} and corresponds to the glass transition temperature T_g^{PI} of PI blocks as indicated by the arrow. Again the small difference in the peak location between the shortest SI and the three other SI samples could be due to the small extent of mixing in the interphase, as explained above. Finally the peak appearing in the intermediate temperature range is strongly dependent on M_{PI} and is due to the normal mode of PI blocks.

IV-2. Frequency dispersion of SI copolymers: In Figure 1, we have attributed the peaks from lower to higher T, respectively, to the segmental and normal modes of PI blocks and to the segmental mode of PS blocks. However, the assignment is rather qualitative, because changes in temperature could induce changes in the microdomain structure, thereby affecting the ϵ'' curve if the temperature is close to or higher than T_g^{PS}. To avoid this difficulty, we can examine the frequency dispersion behavior at

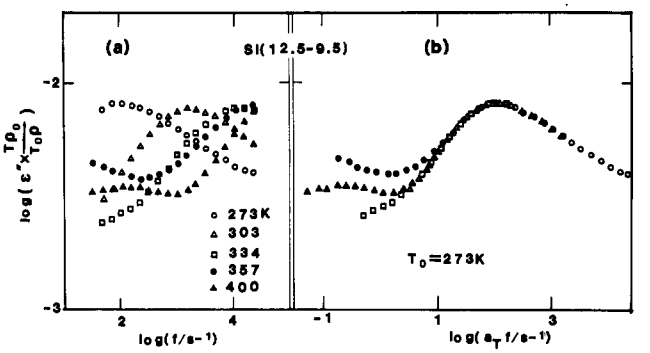

Figure 2. Frequency dependence of the dielectric loss factor of SI(12.5–9.5) at the temperatures indicated: (a) plot of the raw data; (b) the composite curve obtained by a shift along the frequency axis.

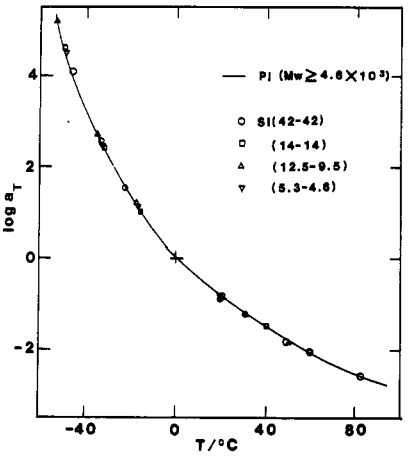

Figure 3. Temperature dependence of the shift factor a_T for the ϵ'' data of the SI copolymers indicated. The solid curve represents the shift factor for bulk PI.

constant temperatures where no changes in the microdomain structure take place.

To make sure whether such a structural change is taking place or not, we examined the thermorheological simplicity. Figure 2 shows the results for SI(12.5–9.5), as an example. In Figure 2a, the ϵ'' curves obtained at five different temperatures are plotted against frequency. To correct for a small change in the dielectric relaxation intensity with temperature, we multiplied ϵ'' by $T\rho_0/T_0\rho$, with ρ being the density and T_0 = 273 K being the reference temperature. Those ϵ'' curves are shifted along the frequency axis in Figure 2b to examine if the superposition holds.

As can be seen in Figure 2b, the data at low temperatures (unfilled symbols) are well superposed on each other, but those at high temperatures (filled ones) are not. This result suggests that the microdomain structure does not change with T at $T < 334$ K but does change at $T > 357$ K for the SI(12.5–9.5) sample. It is quite likely that the microdomain structure is preserved when PS blocks are frozen at $T < T_g^{PS}$ and that some structural changes can occur at $T > T_g^{PS}$. In fact, we found that the critical temperature above which the superposition failed was higher for larger M_{PS} and was fairly close to T_g^{PS}.

On the basis of the above findings, master curves were constructed for the ϵ'' data at temperatures where the superposition was valid. Figure 3 shows the temperature dependence of the shift factor a_T (for T_0 = 273 K) with which the ϵ'' data of the SI copolymers were very well superposed. The solid curve represents the a_T of homo-PI samples,[13] which is insensitive to M_{PI} for $M_{PI} \geq 4.6 \times 10^3$.

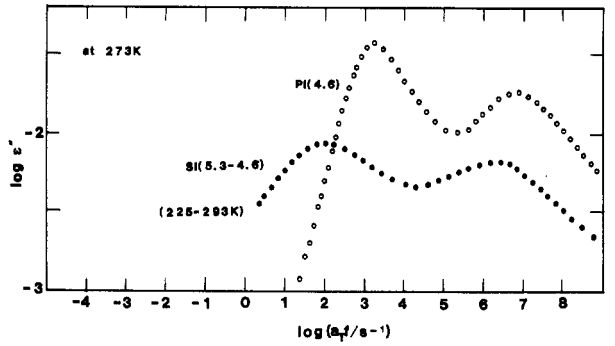

Figure 4. Comparison of the ϵ'' master curves for SI(5.3–4.6) and the precursor PI(4.6) reduced to 273 K. The ϵ'' data at the temperatures indicated in the parentheses were well superposed to obtain the master curve.

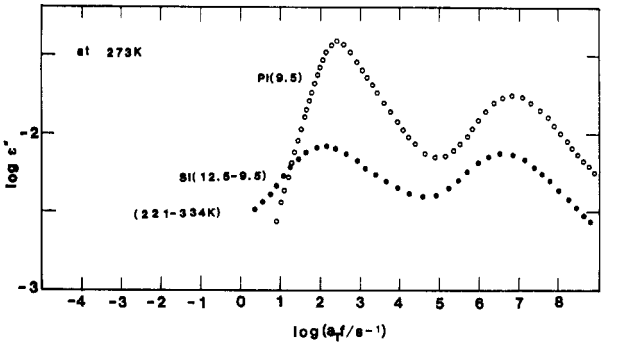

Figure 5. Comparison of the ϵ'' master curves for SI(12.5–9.5) and the precursor PI(9.5) reduced to 273 K. The ϵ'' data at the temperatures indicated in the parentheses were well superposed to obtain the master curve.

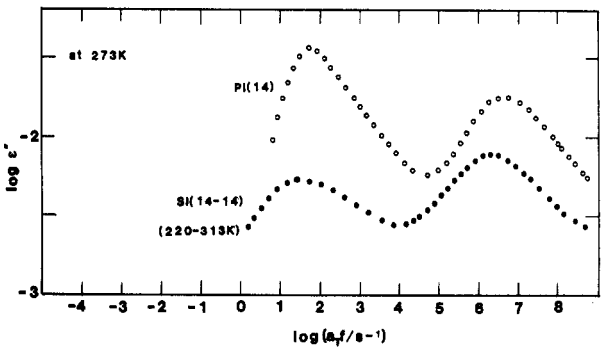

Figure 6. Comparison of the ϵ'' master curves for SI(14–14) and the precursor PI(14) reduced to 273 K. The ϵ'' data at the temperatures indicated in the parentheses were well superposed to obtain the master curve.

As can be seen in Figure 3, the a_T's for SI samples are in good agreement with those for homo-PI precursors. This result suggests that PI blocks are moving in the domains composed of PI segments alone, thereby exhibiting a temperature dependence of the local friction identical with that for homo-PI. This result in turn suggests that the microdomain structure has not changed at the temperatures where the frequency–temperature superposition holds.

Figures 4–7 compare the ϵ'' master curves for four SI samples and the corresponding precursor PI's. The range of temperatures in which the ϵ'' data were superposed is indicated in the parentheses in respective figures.

In Figures 4–7, we first note that both copolymers and presursors exhibit two distinct dispersions at high and low frequencies: The fast dispersion appearing at the high frequency insensitive to M_{PI} is assigned to the segmental mode, while the slow dispersion being retarded with

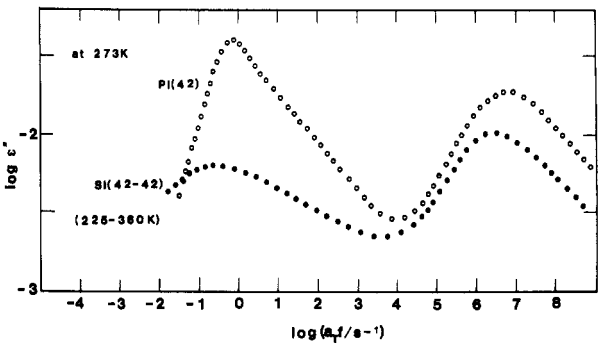

Figure 7. Comparison of the ϵ'' master curves for SI(42–42) and the precursor PI(42) reduced to 273 K. The ϵ'' data at the temperatures indicated in the parentheses were well superposed to obtain the master curve.

increasing M_{PI} can be attributed to the normal mode of PI blocks.

As seen in Figures 4–7, the segmental mode is not very different for SI and the PI precursors. The peak height for the copolymers is smaller by a factor of about $^1/_2$ than that for the precursors, reflecting the 50/50 PI/PS composition of the copolymers. However, the shape of the ϵ'' curves in double-logarithmic scale is nearly the same for the copolymers and precursors, indicating that the relaxation-mode distribution of the segmental mode of PI chains involved is the same. The only difference is the peak location that is slightly shifted for the copolymers to the lower frequency side.

On the other hand, for the normal-mode process, we observe tremendous differences between SI and their PI precursors. First of all, the shape of the ϵ'' curve corresponding to the mode distribution is entirely different: The ϵ'' curve is much broader for the copolymers than for the precursors. Correspondingly, the peak height for the copolymers is significantly smaller than half that for the precursors. These results strongly suggest that the global motion of PI blocks confined in the microdomains is entirely different from that of free PI chains, presumably because the thermodynamic constraints due to the microdomains drastically affect the large-scale motion of the PI blocks.

In the dielectric spectroscopy we often evaluate some sort of average relaxation times, say, τ_s, and τ_n, respectively, for the segmental- and normal-mode processes by

$$\tau_s = 1/(2\pi f_s), \quad \tau_n = 1/(2\pi f_n) \tag{6}$$

where f_s and f_n are the peak frequencies for the respective modes. Figure 8 compares the dependence of τ_s and τ_n on the molecular weight M_{PI} of PI chains involved (=PI blocks for the copolymers).

Here, we have to emphasize that a comparison of τ's for the PI copolymer and precursor does not allow us to make a reasonable estimate for the difference in the relaxation rates *if* the relaxation-mode distribution is quite different. Obviously, if the ϵ'' curves compared have different relaxation-mode distributions, the peaks in those curves give average relaxation times *with different weighting factors* (or with different moments), whatever they may be. Direct comparison of such peak frequencies does not make too much sense.

In this context, we can estimate the difference in the relaxation rate from τ_s for the segmental mode, because the ϵ'' curves have nearly the same shape, i.e., nearly the same relaxation-mode distribution in the segmental-mode region. As can be seen in Figure 8, the τ_s's are insensitive to M_{PI} and larger for SI by a factor of 2 than for the PI precursors.

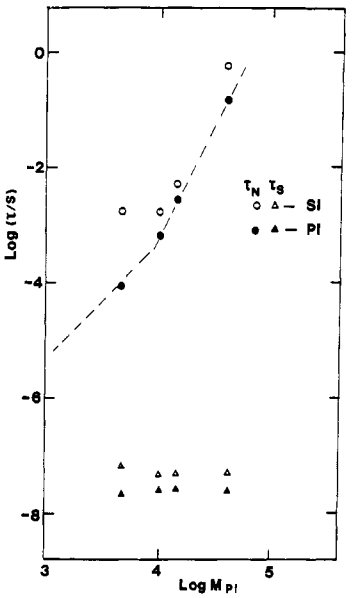

Figure 8. Comparison of the relaxation times for the normal- and segmental-mode processes for SI copolymers (indicated by the unfilled symbols) and precursor PI's (filled symbols). The relaxation times were estimated as $(2\pi f)^{-1}$ from the peak location in the ϵ'' curves demonstrated in Figures 4–7. Note that the comparison of the normal-mode relaxation times of the copolymers and precursors given in this figure is only qualitative, because of the enormous difference in their relaxation-mode distributions. The *longest* relaxation times for the copolymers are expected to be much longer than the relaxation times indicated in the figure. For details, see the text.

For short homo-PI chains, the difference in τ_s is usually attributed to the difference in the glass transition temperature T_g^{PI}. However, as seen in Figure 3, the temperature dependence of the shift factor a_T is the same for block- and homo-PI chains, indicating that T_g^{PI} is the same for those chains. The difference in τ_s observed in Figure 8 is thus not due to the difference in T_g^{PI}. A possible explanation is that the size of a dielectrically observed *segment* is not the same in bulk-PI and in block-PI microdomains. Differences in the thermodynamic environment for those two cases could lead to such a difference. In fact, a change in the segment size was already observed for homo-PI as the thermodynamic environment was changed on dilution.[14]

Turning our attention to the τ_n for the normal modes of SI and their PI precursors shown in Figure 8, we notice that the τ_n for the former is longer than that of the latter by a factor of 3–4 for those of $M_{PI} > 10^4$ and by a factor of $\simeq 15$ for those of $M_{PI} = 4.6 \times 10^3$. Some differences in the dynamics of PI blocks may exist in nonentangled ($M < M_c = 10^4$) and entangled ($M > M_c$) regimes. However, we should be careful to interpret those results, because the normal-mode distribution is so much different for SI and their PI precursors. As observed in Figures 4–7, the ϵ'' curves for SI are only weakly dependent on the frequency f ($\epsilon'' \propto f^{1/4}$) even in the lowest f tail attainable, as opposed to the PI precursors, which exhibit the linear dependence, $\epsilon'' \propto f$ at low f, being characteristic of the terminal zone of any relaxation processes. The weak f-dependence of ϵ'' for SI implies that the longest relaxation time is much longer than the τ_n estimated from the ϵ'' peak frequency. Qualitatively similar behavior, weak f-dependence of dynamic mechanical moduli at low f, was found for ethylenepropylene–ethylene diblock copolymers.[17]

Thermodynamic effect on the global motion of PI blocks: To interpret the findings that the normal-mode distribution for PI blocks is so much broader than that of the PI precursors (cf. Figures 4–7), we seek possible factors leading to such a difference.

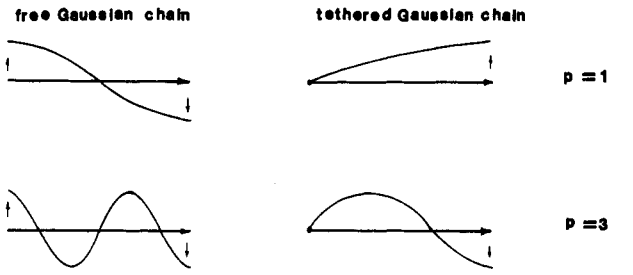

Figure 9. Schematic representation for dielectrically active normal modes for nonentangled type-A Gaussian chains in a free space without (left) and with a fixed end (right). The fundamental and third-order normal modes are shown for those chains with the same length. Note that the wavelength for the pth normal mode is *always* twice longer for the tethered chain than for the free chain. This feature leads to the fact that the longest relaxation time is 4 times longer for the tethered Gaussian chain than for the free chain, but the relaxation-mode distribution is the same for these chains.

First, we consider a tethered type-A Gaussian chain in *free space* and examine if the fixed end can lead to the retarded and broadened dielectric normal-mode distribution. For a nonentangled tethered chain in free space, the longest relaxation time is 4 times longer than that of the free Gaussian chain with the same length, *but the shape of the ϵ'' curve is exactly the same.*[18] This is due to the difference in the wavelength of the slow normal modes for end-grafted and free Gaussian chains as depicted in Figure 9. Obviously the tethered free-chain model cannot explain the broadening of the mode distribution for PI blocks observed in Figures 4–7.

Entanglements among tethered chains could also lead to retarded and broadened dielectric relaxation behavior. However, we have observed such behavior not only for lightly entangled PI blocks in SI(42–44), SI(14–14), and SI(12.5–9.5) samples but also for nonentangled short PI blocks in SI(5.3–4.6). As seen in Figures 4–7, the mode distribution is essentially the same for those four samples. The entanglement effect does not seem to be essential, at least, for PI blocks with $M_{PI} \leq 42 \times 10^3$ examined here.

Another factor we may have to consider is the distribution of lamellar orientation. Because the responses of PI blocks end-grafted on PS lamellae oriented parallel or perpendicular to the electric field could be different, the distribution of lamellar orientation could broaden the ϵ'' curves. However, in the films of SI block copolymers prepared in situ in the capacitance cell by solution casting, the PI lamellae are expected to be almost parallel to the electrodes. Under such a situation the distribution of lamellar orientation would not be important.

Still other possibilities are schematically shown in Figure 10: Figure 10a shows a model in which a PI block chain is end-grafted on the PS domain wall and confined in the narrow space with the width identical with the thickness of the PI lamella, and Figure 10b, the same end-grafted PI block chain subjected to strong thermodynamic interactions with the surrounding end-grafted block chains.

As to the model A, we should note that the behavior of a tethered Gaussian chain is not the same in confined space and in free space: The segment distribution function is distorted in the narrow confined space, thereby removing the Hookian nature from the Gaussian chain to affect the mode distribution.

The model B, we believe, is much more essential to describe the dynamics of microphase-separated block copolymers. As mentioned in the Introduction, each block

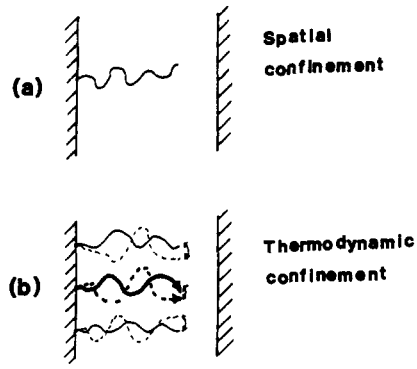

Figure 10. Schematic representation for two types of confinements, which can lead to the retarded and broad dielectric relaxation of the PI blocks in the microdomains. In part b, a particular PI block is indicated by the thick lines. If that PI block is surrounded by dielectrically inert chains such as PB blocks, dielectric response of a single PI block chain can be observed.

chain in the microdomain assumes a configuration strongly affected by the thermodynamic interactions. The motion of such a block chain is then inevitably coupled with the surrounding chains through such interactions to minimize density fluctuation. This possibly leads to retarded and broadened dielectric normal modes.

Behavior of block- and homo-PI chains in SI/SB and PI/PS/SB blends: As explained in Figure 10b, we expect a strongly coupled motion of PI block chains due to the thermodynamic interactions. Thus, we have to first examine if the dielectric response of the PI blocks corresponds to the sum of the contributions of individual blocks. In other words, we have to examine whether or not the cross-correlation for different PI blocks, $\langle z_{p,n}(t)\, z_{q,m}(0)\rangle$ with $p \neq q$ (eq 3), vanishes and eq 3 is reduced to eq 4. For this purpose, we examined blends of SI and SB copolymers with nearly the same styrene-to-diene content ($\simeq$50/50).

For short SI and SB block copolymers with nearly the same characteristics, we expect the PI and PB blocks to be miscible and to form a mixed (PI + PB) lamellar phase against a common PS lamellar phase. In such a mixed phase, some of the neighboring chains of a particular PI block are dielectrically inert PB blocks, as schematically shown in Figure 10b by the thick (for PI) and thin (for PB) lines. Decreasing the PI/PB ratio in the mixed phase (while keeping the (PI + PB)/PS ratio the same), we would be able to observe a response of a PI block moving in a PB domain in a manner probably similar to that in a PI domain. *If* the dielectric response of such a PI block in the PB domain is the same as that in the PI domain, we may conclude that the cross-correlation in eq 3 is not significant for ϵ'' of bulk SI copolymers and that the ϵ'' simply reflects the autocorrelation of the individual PI blocks. Of course, this does not necessarily mean that the PI blocks are moving independently. Instead, since the PI block chains are placed in the thermodynamic field, they are forced to move under the influence of strong thermodynamic couplings from the surrounding chains. A mean-field picture would be valid for such cases to describe the motion of the PI blocks as the motion of a single block chain in an *effective* field.

To examine whether or not the above scheme is correct, we designed the following experiments. We made blends of reasonably short SI(12.9–9.5) and SB(8.6–8.5) samples having nearly the same molecular weight and diene/PS content ($\simeq$50/50). The PI and PB blocks involved appeared to form a mixed lamellar phase, as we see later

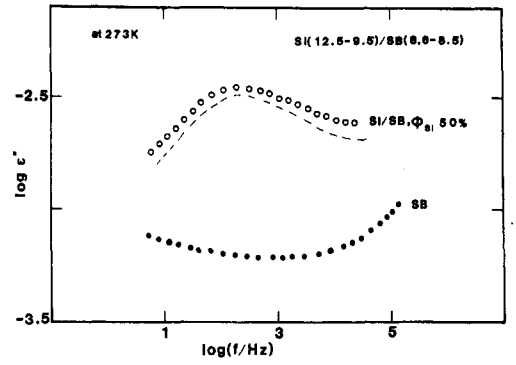

Figure 11. Comparison of the ϵ'' curves of SI(12.5–9.5)/SB-(8.6–8.5) blends with ϕ_{SI} = 50% (unfilled circles) and bulk SB-(8.6–8.5) (filled ones). The dashed curve indicates the $\epsilon''_{PI;b}$ evaluated by eq 7 for PI blocks in the blends.

in Figure 12. For these blends, we have examined if the dielectric response of the PI blocks remains essentially the same with decreasing PI content (or SI/SB ratio).

For comparison, we also examined behavior of ternary blends composed of homo-PI (PI(9.5) and/or PI(4.6)), homo-PS (PS(10)), and SB(8.6–8.5) with keeping the (PI + PB)/PS ratio again at 50/50. These ternary blends are quite similar to the SI/SB binary blends except that the PI chains involved are not end-grafted on the domain wall. Comparing the behavior of these SI/SB and PI/PS/SB blends, we can see in the clearest form the effect of end grafting on the molecular motion of the chains placed in the thermodynamic field.

Figure 11 shows a typical example of the ϵ'' master curve obtained for the SI/SB blend with the SI content ϕ_{SI} = 50% (unfilled circles). The reference temperature was 273 K. Similar to bulk SI copolymers, the ϵ'' curves of the blend were well superposed. This result suggests no structural change to have taken place at the temperatures examined.

As seen in Figure 11, the SB copolymer exhibits almost frequency-independent and very small ϵ'' ($<10^{-3}$; filled circles) at $10 < f\,(\mathrm{Hz}) < 10^5$. This is obviously because PB blocks are not a type-A chain and their global motion is dielectrically inert. On the other hand, the SI/SB blend (unfilled circles) exhibits a prominent peak attributable to the normal mode of the PI blocks. For this blend we have evaluated the ϵ'' due to the PI blocks by a linear blending law:

$$\epsilon''_{PI;b} = \epsilon''_{b} - \phi_{PB}\epsilon''_{PB;b} \tag{7}$$

Here ϕ_{PB} is the volume fraction of PB, and the subscript PI;b stands for PI in the blend, b, the whole blend, and PB;b, PB in the blend. Since the bulk SB chains exhibited a small and almost f-independent ϵ'', we use their ϵ'' data as $\epsilon''_{PB;b}$ in eq 7 to estimate $\epsilon''_{PI,b}$. This was a harmless approximation because the term $\phi_{PB}\epsilon''_{PB;b}$ in eq 7 is a small correction for $\epsilon''_{PI;b}$ anyway. The dashed curve in Figure 11 indicates the $\epsilon''_{PI;b}$ estimated by this way. For other SI/SB blends with different ϕ_{SI} and also for PS/PI/SB ternary blends, ϵ''_{PI}'s (due to either PI blocks or trapped homo-PI) were evaluated similarly.

Figure 12 shows the temperature dependence of the shift factor a_T (unfilled symbols) with which the ϵ'' data were very well superposed for the SB copolymer and SI/SB and PS/PI/PB blends. For these systems except SB, ϵ'' is essentially due to the PI chains. Thus the changes in a_T represent changes in the local friction factor of the PI chains involved in the blends.

In Figure 12, the solid curve indicates the a_T for bulk PB evaluated from the viscosity data.[19] The dashed curve

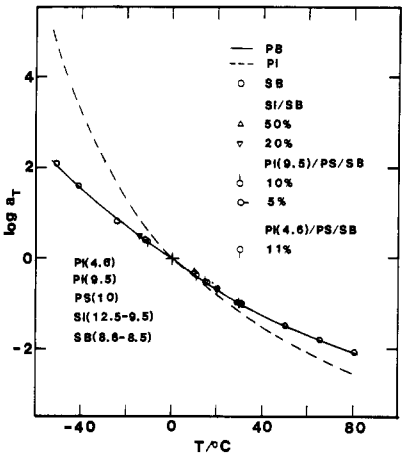

Figure 12. Temperature dependence of the shift factor a_T for the ϵ'' of PI chains in SI(12.5–9.5)/SB(8.6–8.5), PS(10)/PI(4.6)/SB(8.6–8.5), and PS(10)/PI(9.5)/SB(8.6–8.5) blends with varying SI and/or PI content as indicated (open symbols). The solid and dashed curves, respectively, indicate the shift factors for bulk PB and PI.

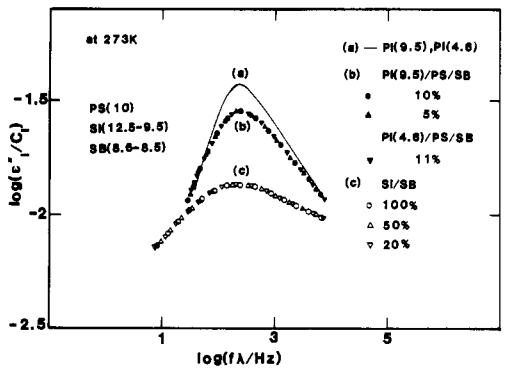

Figure 13. Comparison of the ϵ'' curves for the normal-mode process of PI blocks (unfilled symbols) and homo-PI chains (filled ones), both mixed in the lamellar phase of SB(8.6–8.5). The different symbols correspond to the blends with different SI and/or PI content. The solid curve indicates the ϵ'' curve of bulk PI. Each ϵ'' curve is reduced to the unit mass of PI chains involved, and the frequency is also reduced by the factor λ so that the peak location becomes the same. The λ values are as follows: 1.00 for PI(9.5); 0.14 for PI(4.6); 0.36 and 0.45 for PI(9.5)/PS/SB with ϕ_{PI} = 5 and 10%; 0.069 for PI(4.6)/PS/SB with ϕ_{PI} = 11%; 0.76, 1.20, and 2.09 for SI/SB with ϕ_{SI} = 20, 50, and 100%.

is the shift factor for bulk PI.[14] As can be clearly seen, the shift factors for all the blends fall on the WLF curve for bulk PB, not on the curve for bulk PI. This result strongly suggests that the PI blocks are well mixed with PB blocks at the temperatures examined, and their local friction in the blends is determined by PB blocks.

Figure 13 compares the normal-mode distribution of PI chains in various environments. The ϵ'' curves normalized by the PI concentration C_I were shifted along the frequency axis until the peak locations coincide, so that the mode distribution is compared in the clearest form. The unfilled symbols indicate the response of PI blocks in SI(12.5–9.5)/SB(8.6–8.5) blends with varing ϕ_{SI}. The filled symbols are for homo-PI chains trapped in PS/PI/SB ternary blends. For comparison, the ϵ'' curves for two bulk PI samples, PI(9.5) and PI(4.6), are also shown in Figure 13 by the solid curve.

As can be clearly seen in Figure 13, the relaxation-mode distributions are the same for the PI blocks in SI/SB blends with ϕ_{SI} = 20, 50, and 100% (bulk SI). This result suggests that the ϵ'' data for the SI and SI/SB blends reflect the motion of the individual PI blocks under the given thermodynamic field in the lamellar phase, as explained earlier. Probably some cancellation of the cross product $\dot{z}_{p,m}(t)\, z_{q,m}(0)$ (eq 3) had taken place in the PI domains, as is similar to the cases for bulk PI. Thus, eq 3 can be reduced to eq 4, allowing us to discuss the features of the global motion of a PI block chain in the lamellar phase from the ϵ'' data.

In Figure 13, we also note that the mode distribution is the same for the PI(9.5) and PI(4.6) chains trapped in the PB phase in the ternary blends with $\phi_{PI} \leq 11\%$. The ϵ'' curves for the trapped PI chains (filled symbols) are narrower than those of the PI blocks (unfilled ones). This fact indicates the effect of thermodynamic interaction on global motion to be larger for the PI blocks.

For PI chains unconnected to the domain wall, the thermodynamic requirement of keeping the uniform segment density throughout the microdomain can be satisfied rather easily through displacement of the center of mass without seriously affecting the chain configuration. On the other hand, for the PI blocks with an end-grafted configuration, displacement of the center of mass always accompanies a serious change in the configuration. In other words, the two factors affecting the motion of the PI blocks explained in parts a and b of Figure 10 are not completely independent of each other. Such coupled confinements on the PI blocks may lead to the difference between ϵ''_{PI} in the binary (unfilled symbols) and ternary blends (filled ones) observed in Figure 13.

Another interesting point worthwhile to be noted in Figure 13 is that the ϵ'' curve of the short PI chains in the ternary blends (filled symbols) is not very much but certainly broader than that in bulk PI (the solid curve). This is presumably due to the thermodynamic interaction in the lamellar phase, the factor depicted in Figure 10b. Although the PI chains are not covalently bonded to the domain wall, they have to move in the thermodynamic field created by the (dielectrically unobservable) PB blocks.[20]

V. Concluding Remarks

The results obtained in Figure 13 suggest that the global motion of PI blocks in microdomains can be examined by dielectric spectroscopy even though the static correlation of the configuration exists for different blocks. Two types of confinements, the spatial and thermodynamic confinements, affect the global motion of the PI blocks as well as of homo-PI chains in the microdomains: The effects are larger for PI blocks than for homo-PI chains. Detailed and quantitative discussion on the mechanism(s) of how these confinements affect the global motion of those PI chains is an interesting and important problem remained, which we will discuss in future work.

References and Notes

(1) See, for example: Hashimoto, T. In *Polymer Alloy*; Kotaka, T., Ide, F., Nishi, T., and Ogino, K., Eds.; Kagaku Dojin: Tokyo, 1981.
(2) Meier, D. J. *J. Polym. Sci.* **1969**, *C26*, 81.
(3) Helfand, E.; Wasserman, Z. R. *Macromolecules* **1976**, *9*, 829; **1978**, *11*, 960.
(4) Molau, G. E. In *Block Copolymers*; Aggarwal, S. L., Ed.; Plenum Press: New York, 1970.
(5) See, for example: Holden, G. In *Block and Graft Copolymerization*; Ceresa, R. J., Ed.; Wiley: New York, 1973; Vol. 1.
(6) Kotaka, T.; Watanabe, H. In *Current Topics in Polymer Science*; Ottenbrite, R. M., Utracki, L. A., Inoue, S., Eds.; Hanser Publishers: New York, 1987; Vol. II, and references therein.
(7) Stockmayer, W. H. *Pure Appl. Chem.* **1969**, *15*, 539.
(8) Adachi, K.; Kotaka, T. *Macromolecules* **1984**, *17*, 120.
(9) Adachi, K.; Kotaka, T. *Macromolecules* **1985**, *18*, 466.
(10) Adachi, K.; Kotaka, T. *J. Soc. Rheol. Jpn.* **1986**, *14*, 57.
(11) Adachi, K.; Kotaka, T. *Macromolecules* **1987**, *20*, 2018.

(12) Adachi, K.; Kotaka, T. *Macromolecules* **1988**, *21*, 157.
(13) Imanishi, Y.; Adachi, K.; Kotaka, T. *J. Chem. Phys.* **1988**, *89*, 7585.
(14) Adachi, K.; Imanishi, Y.; Kotaka, T. *J. Chem. Soc., Faraday Trans. 1* **1989**, *85*, 1083.
(15) Cole, R. H. *J. Chem. Phys.* **1965**, *42*, 637.
(16) Allen, V. R.; Fox, T. G. *J. Chem. Phys.* **1964**, *41*, 337.
(17) Rosedale, J. H.; Bates, F. S. *Macromolecules* **1990**, *23*, 2329.
(18) We can easily find this result from an autocorrelation function for the tethered and free nonentangled chains calculated by a Rouse equation with appropriate boundary conditions. See, for example: Graessley, W. W. *Adv. Polym. Sci.* **1982**, *47*, 111.
(19) Colby, R. H.; Fetters, L. J.; Graessley, W. W. *Macromolecules* **1987**, *20*, 2226.
(20) For the PI(9.5) and PI(4.6) chains, the spatial confinement indicated in Figure 10a may, in principle, also broaden the ϵ'' curve shown in Figure 13. However, the ϵ'' curves of those two PI chains are indistinguishable, despite the fact that the spatial confinement is stronger for the longer PI(9.5) chain. Thus, the effect of spatial confinement appears to be rather minor for the motion of those PI chains examined, probably because they are not too long as compared to the domain width.